GA–A24838

CONTRIBUTIONS FROM THE NEUTRAL BEAMLINE IRON TO PLASMA NON-AXISYMMETRIC FIELDS

by
J.L. LUXON

MARCH 2005

GENERAL ATOMICS

DISCLAIMER

GA–A24838

CONTRIBUTIONS FROM THE NEUTRAL BEAMLINE IRON TO PLASMA NON-AXISYMMETRIC FIELDS

by
J.L. LUXON

Work supported by
the U.S. Department of Energy
under DE-FC02-04ER54698

GENERAL ATOMICS PROJECT 30200
MARCH 2005

GENERAL ATOMICS

In this memo, a characterization of the contributions to the non-axisymmetric fields in the plasma owing to the presence of substantial iron components in the neutral beamlines will be described. These fields are often described as "error fields" because they deviate from the expected axisymmetric fields of the tokamak and because they are thought to cause anomalous MHD behavior in the plasma. Once this characterization is in hand, an upper limit will be put on the predicted change in the non-axisymmetric field. Although the fields affecting the plasma are typically of order, e.g., $m,n = 2,1$, modeling of these fields is difficult and the sources will be characterized by their $n=1$ and $n=2$ components on the magnetic axis as is typically done in such studies (see e.g., Ref. 1). The four beamlines are arranged somewhat symmetrically around the tokamak (Fig. 1) and most of the contribution to the error field is $n=2$ and $n=4$, although a small $n=1$ contribution is expected because two of the beam lines are mounted above the midplane and two below and this is not symmetric. The $n=2$ data from the 2001 in-vessel magnet measurements [1] are used to put an upper limit on the size of the magnetic dipole for each beamline. This works well because the other contributions to the $n=2$ fields are modest. Finally, the impact of the proposed rotation of one beamline from the co- to the

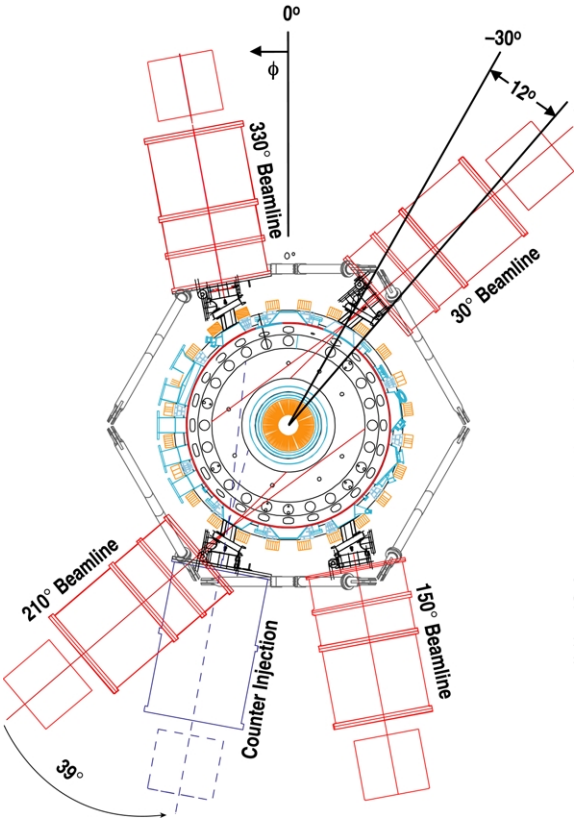

Fig. 1. A top view of DIII–D (1986–2004) showing the four beamlines in the co-injection location. 0 deg is at the top of the page in both a right-handed coordinate system and in the machine (cw) coordinate system.

counter-direction is estimated. In all cases, the contributions of the beamlines to the $n=1$ error field appear small although the rotation of one beamline will likely increase it by a small amount. After the rotation of one beamline has been completed, an assessment of the additional contribution to the error field can be made using the toroidal saddle loop array; if data from an E-coil only shot taken before the rotation is subtracted from the same data after the move, the change in $n=1$ contribution can be assessed.

The four beamlines are arrayed around DIII–D as shown in Fig. 1. They are located at –30, –150, –210, and –330 deg; here a right-hand coordinate system is used and the components are characterized using their location in the DIII–D coordinate system with a minus sign. The beamlines are rotated from radial to inject in the ccw direction with a typical pivot of ~ –12 deg in the horizontal plane with respect to a major radius. The beamlines at –210 and –330 deg are mounted in the upper configuration with the centerline of their mechanical components ~30 cm above the mid-plane. The other two have their centerline ~30 cm below the midplane. This produces an $n=1$ field contribution, but estimates are that it is small.

The beamlines have five major iron components (Fig. 2): the bending magnets located in the second spool from the front, the finger shield region behind the bending magnet, the neutralizer shield, the source shield at the back, and the rather substantial support stand, which extends from just under the front of the main beamline cylinder to the rear. The bending magnet and the source shield likely exclude magnetic flux from their entire volume and are easy to characterize. The finger shield likely effectively shields the z component of the field. The neutralizer is considerably smaller and is ignored. The stand is an open structure and much more difficult to evaluate, but the potential contribution appears comparable to others. These components are summarized in block form in Fig. 3.

In the previous analysis of the in-vessel magnetic data, individual iron components were modeled with the dipole model developed by Jim Leuer and myself in the Microsoft® Excel version of the analysis code for the magnetic data taken with probes inside the vessel in 2001 (see Ref. 1 for details). This code models an iron sphere of radius a with a coil of radius a (area $\propto a^2$) and current proportional to a and the exciting magnetic field B_{source} is the field that the iron is immersed in. For a non-spherical enclosed volume, the equivalent volume is used. Thus the field of the dipole can be written as

$$B_d \propto F\ B_{source}\ a^3/r^3$$

where F is a multiplier to account for elongation or any other weight factor. As I recall, if the magnetic object is elongated along the direction of the exciting field, this model underestimates the dipole strength, i.e., $F \gtrsim 1$. When comparing experiments to models, F also accounts for errors in estimating the volume (a) or location (r)of the dipole.

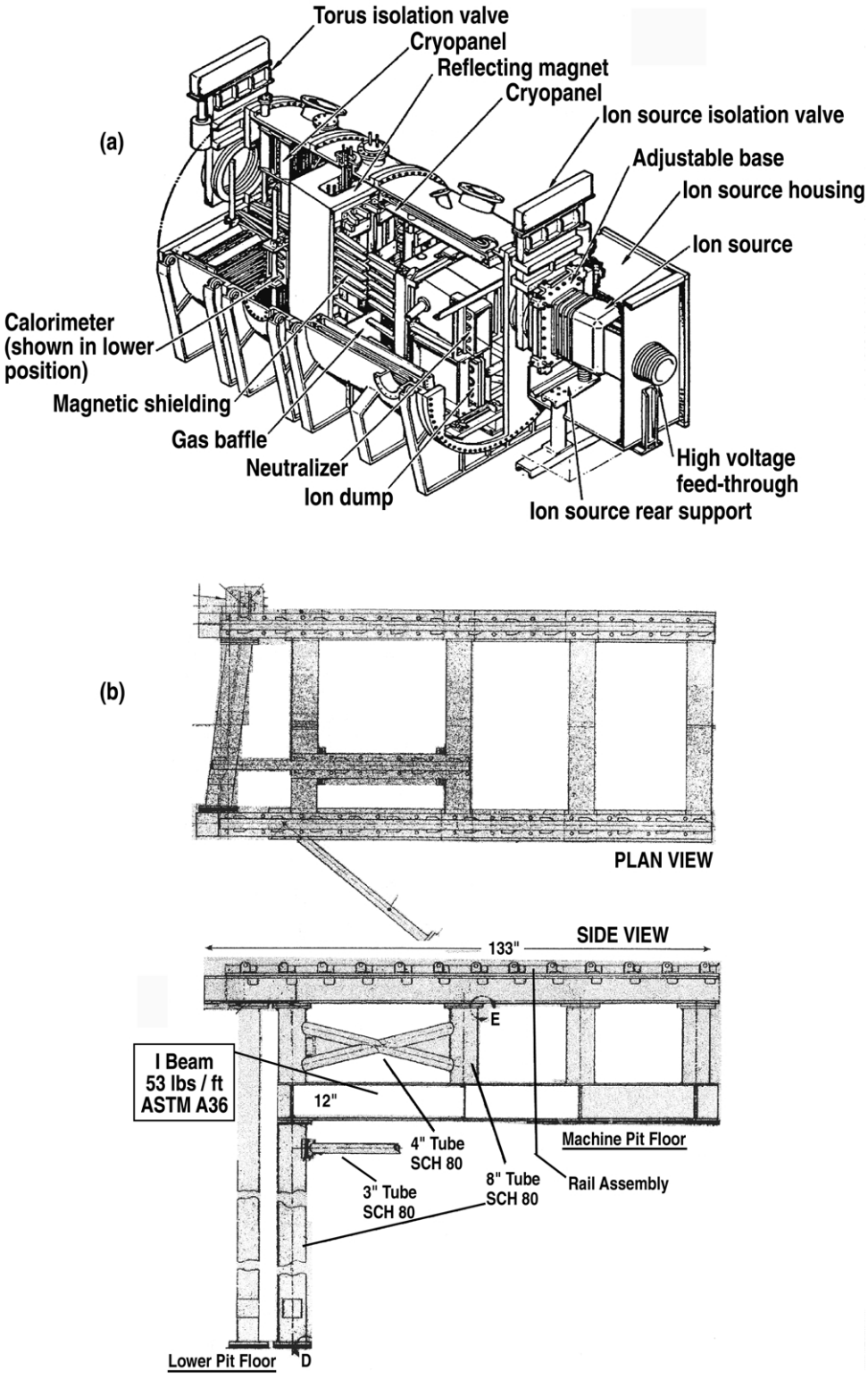

Fig. 2. (a) An isometric view of a DIII–D neutral beamline showing the internal components. Key iron components are identified as Reflecting Magnet, Magnetic Shielding, Neutralizer, and Ion Source Housing. Note that the magnetic shielding fingers just in front of the neutralizer (near the end of the arrow marked Gas Baffle) were not installed. (b) Plan and Side views of the steel beamline stand.

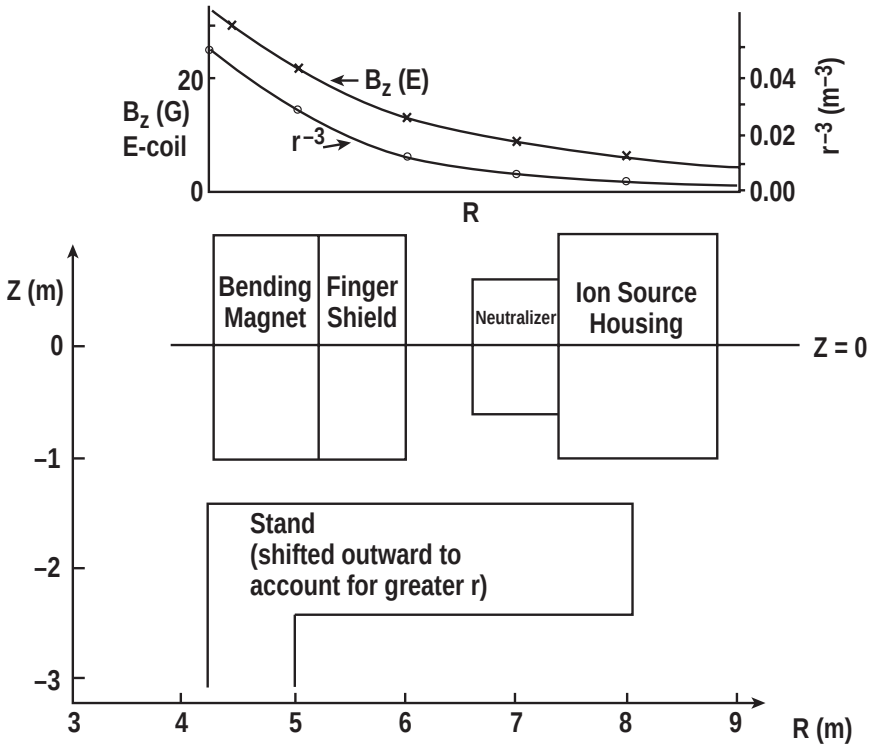

Fig. 3. A block diagram of the iron beamline components showing their location (R,z) in toroidal coordinates. Inset above is the calculated field of the E-coil for I_E = 10 kA/turn and r^{-3} measured to the magnetic axis (R_0 = 1.7 m).

Primarily, the E-coil error field data will be used to evaluate the contributions to the $n=2$ field because of the relative clarity of the data. At the top of Fig. 3, the radial dependence of the exciting field at the midplane using the E-coil with a current of 10 kA/turn is shown. Also shown is the characteristic r^{-3} fall off of a dipole from the magnetic axis. At the midplane, the E-coil field is in the z direction. The contributions from the beamline internal components add arithmetically in the z direction since they are aligned perpendicular to B_z. Initially, we will consider contributions dominantly in the z direction since that is the direction of the E-coil external field near the midplane. Considering both the r^{-3} dependence and falloff in the source field exhibited in Fig. 3, the contribution of the bending magnet is likely dominant amongst the beamline internal components, although the finger shield and ion source housing together could approximately equal the contribution of the bending magnet (implies $F > 2$).

The beamline support stand [Fig. 2(b), courtesy of Jeremy Phillips) is much more difficult to characterize. The stand stretches from the front of the beamline, where the exciting fields are strong and the distance to the plasma small, to the back of the beamline where just the opposite holds. The enclosed volume in the R direction is significant and the substantial length implies a large multiplier. My estimates of this from various viewpoints indicate that it could have comparable contribution to the bending magnet.

Fortunately, all of these contributions for a given beamline are at essentially the same toroidal angle. For simplicity, the bending magnet alone will be modeled and the other contributions will be accounted for by the factor F. The bending magnet is 2 m high by 1 m wide by 0.8 m radially, oriented with its long dimension in the z direction. It has a volume of 1.6 m^3 and the equivalent spherical radius is a = 0.7 m. It is located at 4.9 m and with the first one located at ~18 deg toroidally. Note that this represents the "330 deg" beamline (DIII–D coordinates) located at 30 deg in a right-handed system and shifted to 18 deg by the –12 deg pivot of the beamline. Also note that the toroidal angle for the iron components in the beamlines varies from –5 deg at the front of the stand to –15 deg at the ion source.

The dipole field at the plasma major radius of an iron volume with a = 0.7 m located at r_d = 4.9 m has been calculated by the code and is shown in Fig. 4. The dipole was positioned at Z = –0.5 m and the measurement array was taken to be in the midplane (Z ~ 0) position. The exciting field is F6B at 1500 A to mimic the field of the E-coil at 20,000 A (10 kA/turn). (The model does not handle the multi-component E-coil.) The dipole is placed at 180 deg to center it in the figure.

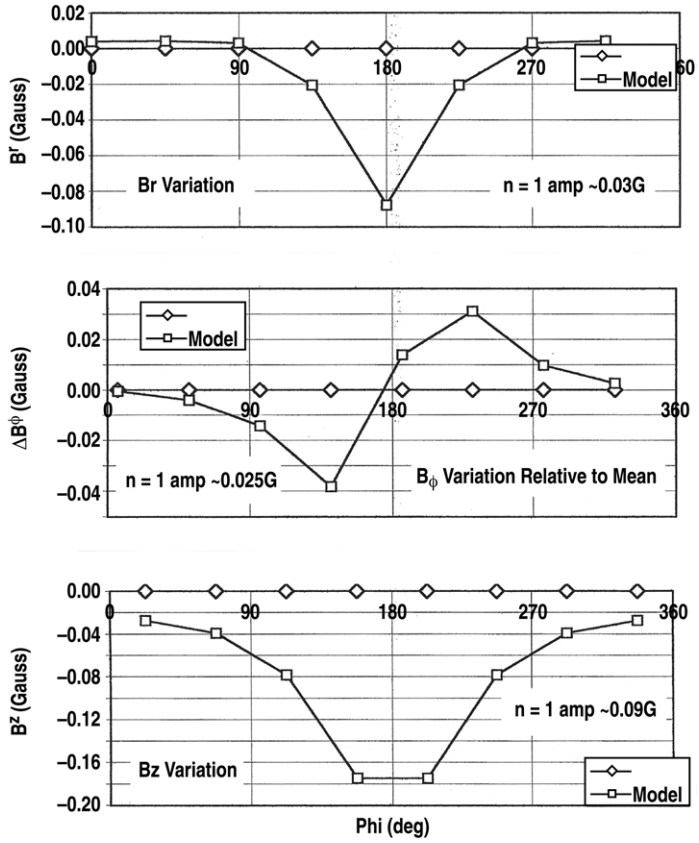

Fig. 4. The fields at R = 1.7 m, z = 0 as a function of toroidal angle ϕ of an iron dipole of radius a = 0.7 m located at R = 4.9 m, z = –0.5 m and ϕ = 180 deg. The exciting field B_z = 22 G is provided by F6B, and is equal to the field for the E-coil with I_E = 10 kA/turn.

The peak field contributions are 0.15 G or less. Also note the characteristic phase relationship between the components. An $n=1$ fit to the largest component (B_z) would have an amplitude of ~0.06 G.

The $n=2$ field for four dipoles at the four beamline locations can be obtained by superposition and is shown in Fig. 5. Here the dipoles were placed at 18, 138, 198, and 318 deg to include a 12 deg shift for co-injection. The resultant $n=2$ amplitude is <0.05 G for all three components. This is essentially a quadrapole field owing to the fact that the beamlines are not evenly spaced around the machine. The higher order components ($n=4,\ 6$) cannot be readily assessed due to the coarseness of the toroidal scale. If the beamlines were set for perpendicular injection, (pivot angle = 0), the expected phase for B_z or B_R would be 0 deg (180 deg) or 90 deg (270 deg), and for B_T it would be 45 deg or 135 deg. For the case shown in Fig. 5, the $n=2$ field is expected to have a phase of ~78 deg for the beamlines shifted by an average toroidal angle of 12 deg.

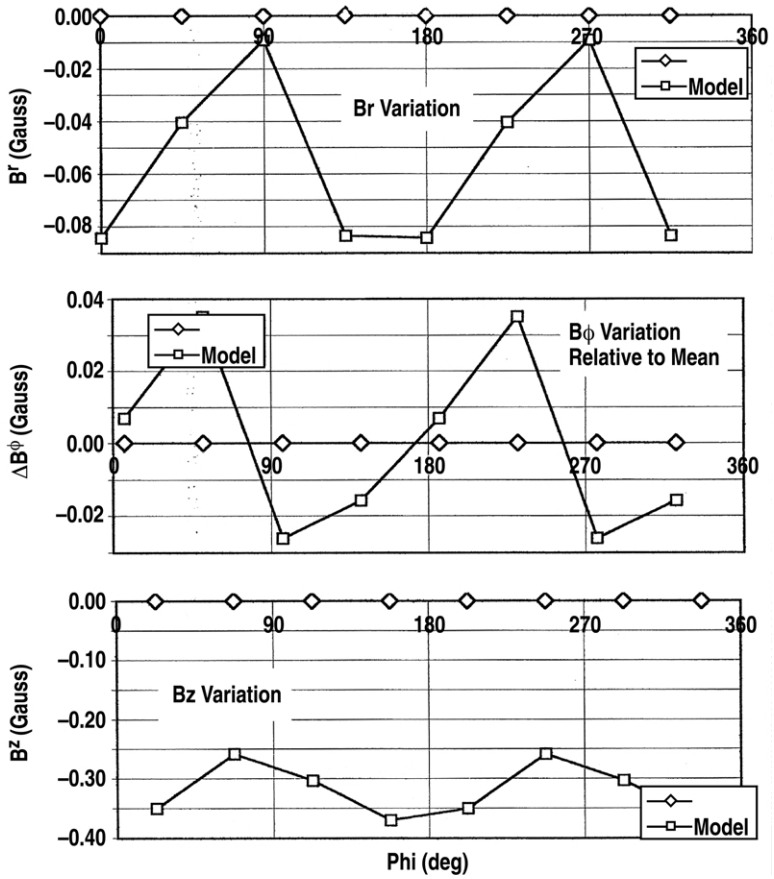

Fig. 5. The combined field of four dipoles located at R = 4.9 m, z = –0.5 m, and ϕ = 18, 138, 198, and 318 deg to represent four beamlines arrayed around the machine. Note the strong $n=2$ component.

The E-coil data from the in-vessel error field measurement set is attractive for evaluating this model. The background ($n=0$) field at the measurement apparatus from

the E-coil is small, resulting in less noise. The E-coil is made up of many individually fabricated and placed turns so that the intrinsic $n = 2$ field is hopefully small. The $n = 2$ error field data at the three different elevations, –0.75 m, 0.05 m, and +0.75 m, are displayed in Fig. 6. The data points are the residual data after the small $n = 1$ component (0 to 0.8 G) was removed, and the smooth curve is the $n = 2$ fit to the data shown. The amplitude and phase of the fit is displayed in the top of the box. Note that an $n = 2$ fit to the data including the $n = 1$ would produce the same result, but the visual presentation would show more data scatter although this scatter would not be indicative of the quality of the fit (because it contains $n = 1$).

The $n = 2$ error field data can come from a combination of a number of factors including dipole contributions from various of the iron beamline components (these can change depending on the elevation of the measurement), anomalies in the coil construction, or other iron components in the vicinity (unlikely for $n = 2$). Since we are only attempting to set an upper limit on the contributions of the beamline iron to the magnetic field, we will only use the E-coil data to set an upper limit on the strength of the beamline contribution to the $n = 2$ field. We will then use that result to evaluate the $n = 1$ field expected after the rotation of one beamline. More detailed analysis of the $n = 2$ data is presented in the Appendix.

As seen in Fig. 6, the E-coil $n = 2$ data has an amplitude of ~0.4 G or less. Comparing to the $n = 2$ model in Fig. 5, the amplitudes differ by ~8 and thus the unknown factor F = ~8 or less. That is, the measured $n = 2$ E-coil data is 8 times larger than estimated from the initial dipole model. The factor $F \sim 8$ represents an upper limit of the contribution of the beamlines to the E-coil $n = 2$ field.

The $n = 2$ error field data from the F-coils is more muddled apparently owing to competing contributions from small distortions in the coils themselves. The presence of the beamline contributions can be seen from a correlation in the phase of the $n = 2$ component for the outer F-coils with the expected phase of the beamline contribution (Fig. 7). However, if one tries to find consistent evidence of a single quadrapole that fits all of the data sets, the data does not support this. This is an indication that the level of the contribution of the Beamline quadrapole is at about the average value of the $n = 2$ field contributions observed for the outer F-coils. This level is 0.2 to 0.4 G for F-coils excited with 1800 A (not shown). This field is similar to or perhaps smaller than the $n = 2$ field seen in the E-coil data. Recalling the earlier statement that a current of 1500 A in F6B (and thus, roughly, all of the outer F-coils) produces roughly the same exciting field (B_z = 22 G) at the dipole location as a current of 10 kA/turn in the E-coil, it can be concluded that the phase and amplitude of the $n = 2$ field from the F-coil error field related data is consistent with a neutral beam related quadrapole. In addition, the amplitude is consistent with $F < 8$. This consistency from the F-coils is important because it eliminates the possibility that there is an unfortuitous cancellation of the external (quadrapole) and internal (coil self fields) contributing to the E-coil $n = 2$ field.

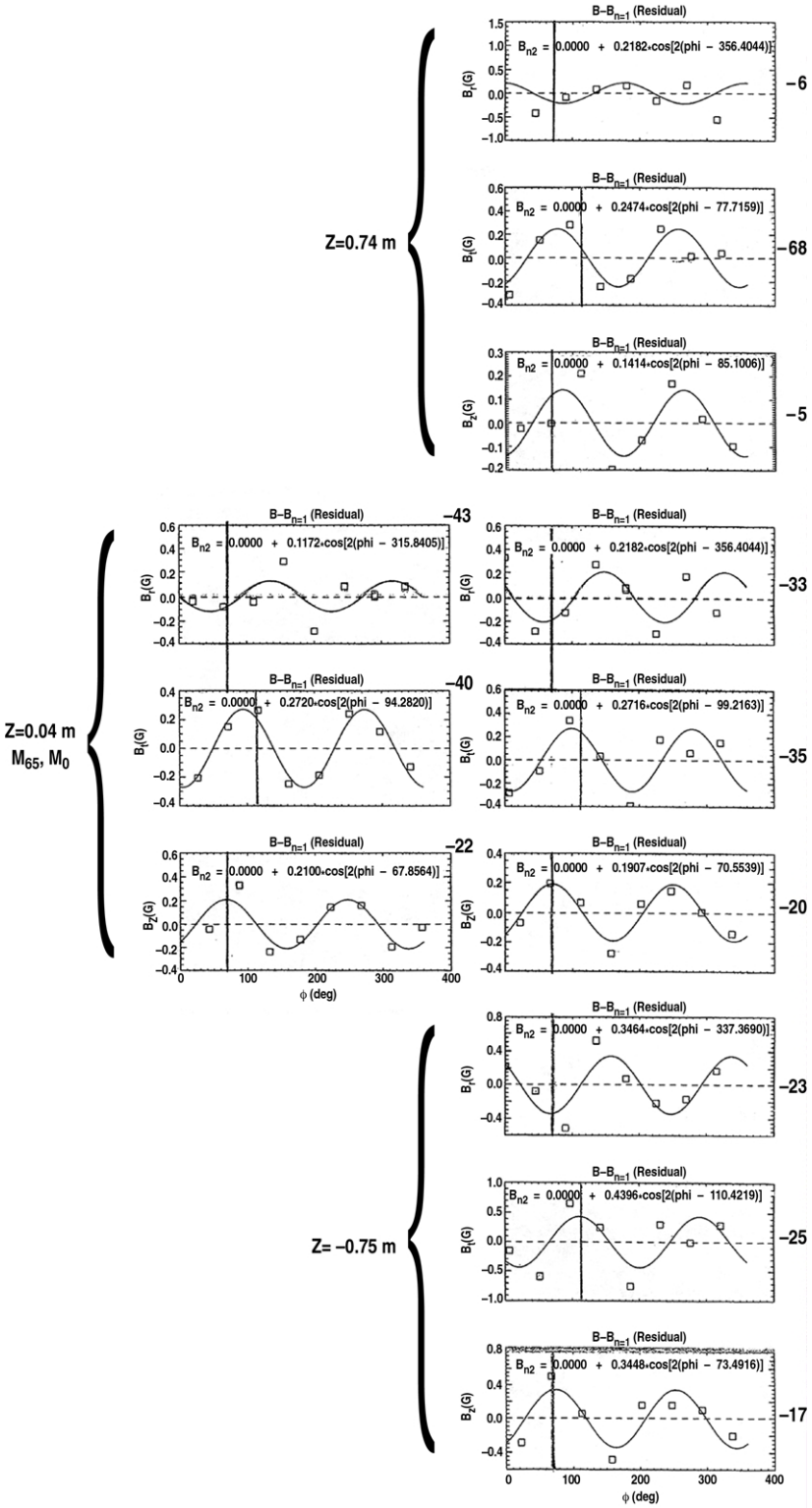

Fig. 6. The $n = 2$ E-coil error field data for measurements made at R = 1.7 m and 10 kA/turn E-coil current. It is displayed for each measurement elevation and two apparatus angles (0 and 65 deg) for the z = 0.04 elevation. The numbers to the right of each figure are the implied phase shift if the fields are related to a quadrapole in the region outside the B-coil.

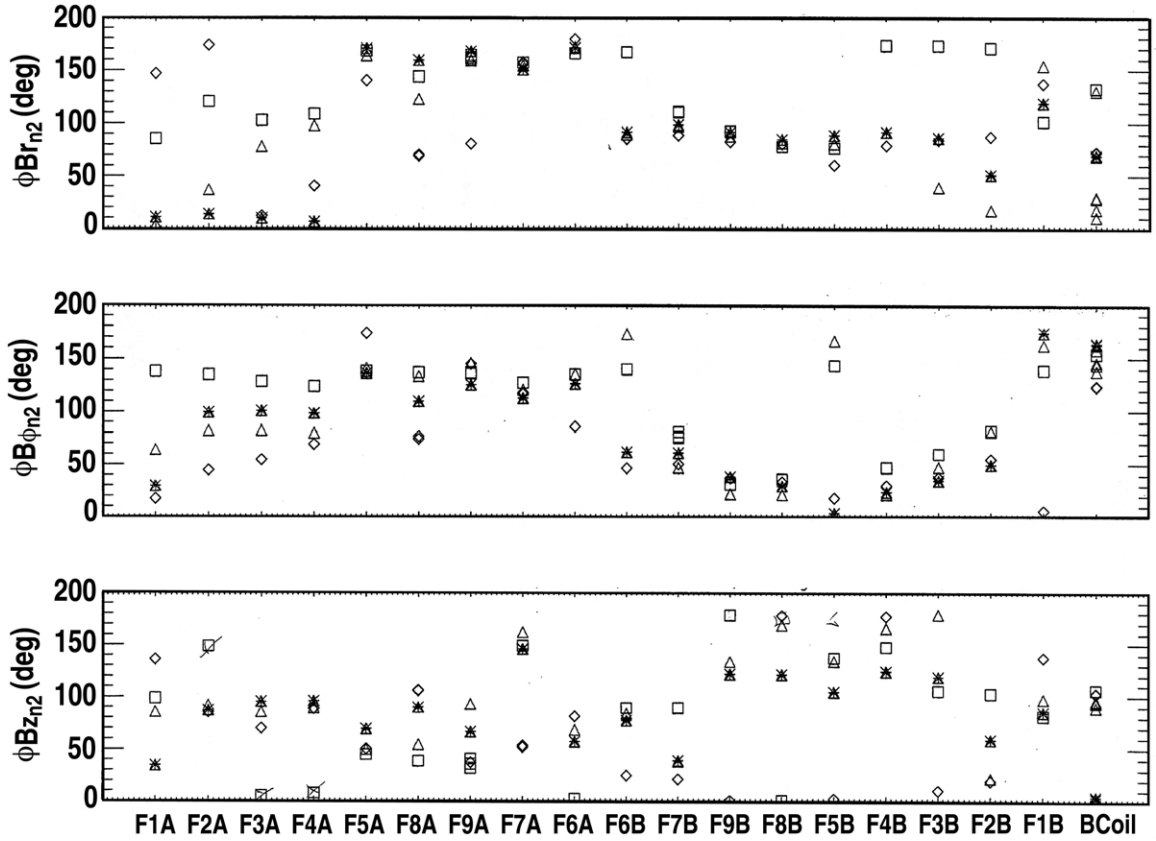

Fig. 7. A summary of the F-coil error field $n = 2$ data measured at R_0 = 1.7 m for several elevations : z = –0.74 m, Δ: z = 0.04 m, ◊: z = +0.75 m, and *: z = 0.04 m (and reference phase 65 deg). The correlation is evidenced from the fact that many of the outer coils (F8A-F6A-F6B-F8B) are characterized by the same phase. Note that since $n = 2$, only the range 0 deg to 180 deg is meaningful and that points plotted near 0 deg could just as easily have been plotted near 180 deg.

From this data, we can conclude that an upper limit on the magnetic contribution of each beamline is given by a dipole with a = 0.7 m and F = 8 located at R = 4.9 m. That F is as large as 8 is not unreasonable since initially only the bending magnet was modeled whereas the combined shield volume is several times larger and the elongation factor is likely >1 for several of the components. On the other hand, a more likely value is F = 4.

It is appropriate to compare the fields estimated here to the measured error fields in the machine. These are given in Fig. 8, which is taken from Fig. 12 of Ref. 1. Here the values of the $n = 1$ components of B_z and B_R are given for all of the F-coils at a current of 2 kA and the for E-coil over the full range of current.

If we assume the present beamline configuration causes no problems for plasma operations, then we can model the effect of rotating one beamline from co- to counter-direction as a pair of opposing dipoles, the first to account for the removal of the existing beamline, and the second to account for the placement in the new position. These dipoles

are separated toroidally by 2 × 12 deg =24 deg. Examining the data for a single dipole in Fig. 4, it can be seen that there will be substantial cancellation between these two dipoles and the resultant $n=1$ field contributions will be less than those of a single dipole. A rough calculation gives B_{1R} = 0.1 G and B_{1z} = 0.32 G as upper limit for an exciting field of 22 G (E-coil current of 20 kA). Comparing these results to Fig. 8 gives encouragement that the expected beamline error fields are small.

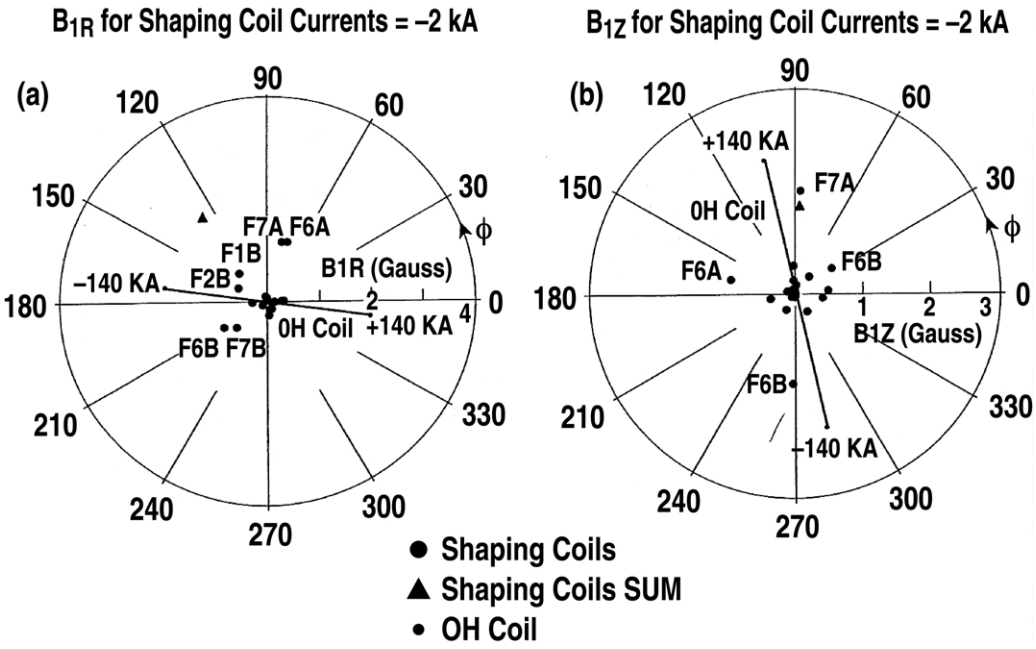

Fig. 8. The measured values of the $n=1$ field components B_{1R} and B_{1Z} for the F-coils (I_F = 2 kA) and E-coil (with total current ranging from I_E = –140 kA to +140 kA).

More accurately, the error fields due to the beamlines are determined by the total field from the plasma, ohmic coil, and all of the F-coils. At high plasma currents, there is considerable cancellation. A limiting example is that of a very low plasma current at full E-coil current. In this limit, we see from Fig. 8 that the field B_{1z} due to the rotation of the beamline would be comparable (but at a different phase) to the E-coil B_{1z} field.

The upper limit for the change in the error field expected for the rotation of one beamline can also be estimated for past discharges using the field calculated using EFIT at the beamline. The exciting field at the beamline center for a sample of discharges is summarized in Table 1. From this it can seen that the field is roughly up/down symmetric $[B_R(z=0)\sim 0]$ and thus $B_z(-1)\sim B_z(+1)$ and $B_R(-1)\sim -B_R(+1)$ [I requested $z=1$, instead of $z=-1$]. From this data, the exciting field at the midplane is estimated to be no more than 100 G at 1 MA. This corresponds to an upper limit on the change in the $n=1$ field in a 1 MA discharge of $B_{1z}\le 1.5$ G at R_0. These results also show that the radial exciting can be significant off of the midplane, but they are not judged to be so large that the error fields would exceed the estimated upper limit.

Comparing to Fig. 8, it can be seen that the $n=1$ field from a beamline after rotation should not exceed that of the most out of place F-coils. The fields of these individual coils are not known to cause a problem.

Table 1
Magnetic Field at the Beamline Center for Four Discharges R = 4.9 m
(Data courtesy of L. Lao)

Discharge	T (s)	I_p (MA)	I_E (kA)	B_R (G) $z=0$	B_R (G) $z=1$ m	B_z (G) $z=0$	B_z (G) $z=1$ m
115863	1500	1.2	0	2.4	–35	61	51
115863	5800	1.2	42	2.9	–48	91	79
103158	1300	1.2	0	–3.9	–31	46	29
88613	2100	1	70	–1.2	–51	93	79

These results may also be put into perspective by comparing to the effect of the $n=1$ coil iron core that was previously removed. Here B_{1R} was larger than B_{1z} (owing to its location above the plasma region) and $\Delta B_{1R}/I_E$ = 0.025 G/kA, comparable to the expected value from the rotation of one beamline. The removal of this core had no observable effect on plasma operation. Thus, the dipole resulting from rotation of the beamline would have a comparable to or smaller effect than the removal of the $n=1$ coil.

Finally, these upper limits on the field resulting from the change in the beamline position can be compared to the "missing" error field contribution from RWM and LM experiments summarized in Ref. 1. This field was characterized by an $n=1$ equivalent field B_1 ~ 25 G, and it had a significant effect on plasma operation. The upper limit on the $n=1$ field expected due to rotating a beamline is under 10 % of this and only at high E-coil current.

After the rotation of the beamline, the actual change in the $n=1$ field can be assessed by comparing the E-coil field at the saddle loop arrays before and after the rotation. Once the fields are normalized to the same E-coil current and subtracted, the resulting $n=1$ component is indicative of the change. The phase is expected to pass through zero at the location of the rotated beamline. A more detailed calculation could then be done to compare to the data at the magnetic axis or a Fourier expansion for the field on a flux surface could be done.

In summary, the iron in each beamline has been characterized by a dipole with characteristic dimensions of the bending magnet — a large easily characterized piece of iron in the highest field region. This technique is an accepted technique for simple models of iron components and was used successfully in modeling the in-vessel magnetic measurements (Ref. 1). The elongated shape of the bending magnet and the contributions

of a number of other beamline iron components are included as a multiplicative factor F. This is realistic since all of these components are at essentially the same toroidal angle. Owing to the symmetry of the present four beamline installation, the major contribution to the fields in the plasma chamber is expected to be $n = 2$ in character. The E-coil and F-coil $n = 2$ data was used to set an upper limit on the fields owing to the beamline iron with the result $F < 8$ (although $F = 4$ is more likely).

Using this result, a dipole model for the change in the rotation of one beamline to inject in the opposite direction was constructed using the characteristic dimensions of the single dipole with $F = 8$. The upper limit on the resultant $n = 1$ field is comparable to the contributions of some of the other machine components. However, based on three different measures, it is not expected to have a noticeable effect on plasma operations. The $n = 1$ field resulting from the beamline rotation can be evaluated using the present saddle loop arrays applied to (E-coil) data taken before and after the change.

ACKNOWLEDGMENT

This work was funded by the Department of Energy under DE-FC02-04ER54698. Thanks to Mike Schaffer for reading of the manuscript.

REFERENCES

[1] Luxon, J. L., M. J. Schaffer, et al., “Anomalies in the applied magnetic fields in DIII–D and their implications for the understanding of stability experiments,” Nucl. Fusion **43** (2003) 1813.

APPENDIX

A careful comparison of Fig. 5 and Fig. 6 shows that the $n = 2$ E-coil measured error field does not exhibit the same phase relationship between B_R, B_z, and B_ϕ suggested by the vertical quadrapole model. The measured B_R and B_z components are 90 deg (180 deg /n, $n = 2$) out of phase instead of in phase as in the model. Nevertheless, the measurements at the four different probe array locations have remarkably similar phase relationships, and the amplitude decreases systematically from bottom to top. Note that any external iron dipole would have similar phase relationships (B_R and B_z in phase or shifted 180°/n, and B_ϕ shifted ±90°/n) because there are no significant toroidal exciting fields in a tokamak. The same is true for the $n = 2$ field due to a coil anomaly in the horizontal plane, e.g., an elliptical distortion of a circular turn. The phase relationships of the data set in Figure 6 are more closely those for a radial dipole below z = –0.75 m (below the level of the lowest measurements) and outside the region of measurement. The amplitude decreasing from bottom to top is roughly consistent with this. The estimated best-fit phase for all of the data is ~ –25 ±10 deg. If the beamlines were set along a radius (normal injection) the phase shift would be 0 deg (or 90 deg, since I did not kept track of the absolute direction), and for the beamlines tilted as they presently are, the phase should shift by between ~ –12 deg and 0 deg. It is hard to support a more negative number.

The *radial nature of the apparent fitted dipole* could indicate that the stand has a large role. However, it is hard to justify such a large dipole moment (there are few crosspieces on the stands in the toroidal direction to complete the box and produce a large apparent structure transverse to the radial field). Simple model and a small amount of available data indicate that the field over most of the beamline and stand is largely vertical, leaving little radial exciting field. Thus, the most logical conclusion is that there is an additional coherent $n = 2$ source contributing to the in-vessel data. This could be the result of a small construction anomaly in the coil (e.g., the center post might be slightly elliptical).

Thus, while the coherence of the $n = 2$ E-coil data is distinctive and intriguing, it is impossible to draw a definitive conclusion. This is why this detail has been placed in an appendix and the $n = 2$ data has only been used to set an upper limit on the beamline contributions. In any case, if the E-coil $n = 2$ data is in part due to a significant second source, our estimate ($F < 8$) above is likely an over estimate.